USING REACTIVE TRANSPORT MODELING TO UNDERSTAND FORMATION OF THE STIMSON SEDIMENTARY UNIT AND ALTERED FRACTURE ZONES AT GALE CRATER, MARS. E.M. Hausrath[1], D.W. Ming[2], T. Peretyazhko[3], and E.B. Rampe[4] [1]UNLV, Las Vegas, NV 89154 Elisabeth.Hausrath@unlv.edu, [2]NASA Johnson Space Center, Houston, TX 77058 [3]Jacobs Jets, Houston TX 77058, [4]Aerodyne Industries, Houston, TX 77058

Introduction: Water flowing through sediments at Gale Crater, Mars created environments that were likely habitable, and sampled basin-wide hydrological systems [1, 2]. However, many questions remain about these environments and the fluids that generated them. Measurements taken by the Mars Science Laboratory Curiosity of multiple fracture zones can help constrain the environments that formed them because they can be compared to nearby associated parent material (Figure 1). For example, measurements of altered fracture zones from the target Greenhorn in the Stimson sandstone can be compared to parent material measured in the nearby Big Sky target [3, 4], allowing constraints to be placed on the alteration conditions that formed the Greenhorn target from the Big Sky target.

Similarly, CheMin measurements of the powdered < 150 micron fraction from the drillhole at Big Sky and sample from the Rocknest eolian deposit indicate that the mineralogies are strikingly similar [3, 4]. The main differences are the presence of olivine in the Rocknest eolian deposit, which is absent in the Big Sky target, and the presence of far more abundant Fe oxides in the Big Sky target [3, 4]. Quantifying the changes between the Big Sky target and the Rocknest eolian deposit can therefore help us understand the diagenetic changes that occurred forming the Stimson sedimentary unit.

In order to interpret these aqueous changes, we performed reactive transport modeling of 1) the formation of the Big Sky target from a Rocknest eolian deposit-like parent material, and 2) the formation of the Greenhorn target from the Big Sky target. This work allows us to test the relationships between the targets and the characteristics of the aqueous conditions that formed the Greenhorn target from the Big Sky target, and the Big Sky target from a Rocknest eolian deposit-like parent material.

Methods: We used the reactive transport code CrunchFlow [5] to model the alteration that generated these targets. CrunchFlow has been previously used to interpret weathering on Costa Rica basalts [6-8], California soil chronosequences [9], ocean floor sediments [10], comparing a range of terrestrial settings [11] and Svalbard basalts [6]. CrunchFlow has also been previously used to interpret weathering on Mars [6, 12-14].

We used as model inputs for the formation of the Big Sky target the mineralogy of the Rocknest eolian deposit. This approach of assuming that parent material is similar to recent unweathered sediments has been previously used on Earth [15]. For the Greenhorn target, the mineralogy of the Big Sky target was used. Mineralogies were based on values given in the Planetary Data System (https://pds.nasa.gov/) and [4], excluding minerals present at less than 5% to simplify the model, adjusting total mineral volumes to allow for a 40% porosity based on terrestrial analogs [16], and using basaltic glass as the amorphous component [17]. Transport within the model forming Big Sky was conceptualized as flow with rates consistent with those resulting from compaction [18], and within the model forming Greenhorn was conceptualized as diffusion radiating out from the fracture. Discretization within the model was based on the scale of the observations of Greenhorn and Big Sky mineralogy (the 1.6 cm size of the drill), and model surface areas, solubilities, and dissolution rates were input from the literature.

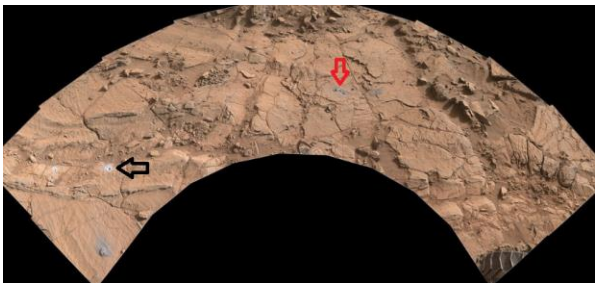

Figure 1. *Image of Big Sky (red arrow) and Greenhorn (black arrow) drill sites, which are outside and inside the altered fracture zone, respectively. Image credit: NASA / JPL / MSSS*

Results and Discussion:

Formation of the Big Sky target.

To interpret the aqueous diagenetic conditions that could form the Stimson sedimentary unit from a Rocknest eolian deposit-like parent material, we compared the model outputs of alteration of the Rocknest mineralogy to the CheMin measurements of the Big Sky target. In particular, we examined 1) the dissolution of olivine, and 2) the formation of Fe oxides, over a pH range of 2-8.

Dissolution of olivine occurred over the entire pH range examined, but magnetite formed only over a pH range of ~ 6-8 (Figure 2). Based on these observations, solutions that formed the Stimson sedimentary unit were likely moderate in pH.

Formation of the Greenhorn target.

Similarly, to interpret the aqueous conditions that formed the altered fracture zones from the bulk Stimson sedimentary unit, we compared the model outputs of alteration of the input Big Sky mineralogy to the CheMin measurements of the mineralogy of the Greenhorn target. The results of our modeling show the dissolution first of pyroxene followed by the dissolution of plagioclase (Figure 3). High sulfuric acid concentrations in input solutions and consequently very acidic conditions (pH = 2) resulted in the precipitation of significant gypsum and amorphous silica in agreement with mineralogical observations of Greenhorn (Figure 3). Under less acidic conditions (pH 3-4), dissolution of the minerals followed a similar trend and significant amorphous silica formed, but less gypsum formed, most likely due to decreased dissolution of the primary minerals. Above pH 4, mineral dissolution occurred, but minimal precipitation of amorphous silica and gypsum was observed. This modeling of Big Sky alteration to Greenhorn shows that mineral dissolution and precipitation under acidic conditions (pH = 2-4, Figure 3) is largely consistent with martian observations, but not mineral dissolution and precipitation occuring under near-neutral and basic conditions (pH 5-8).

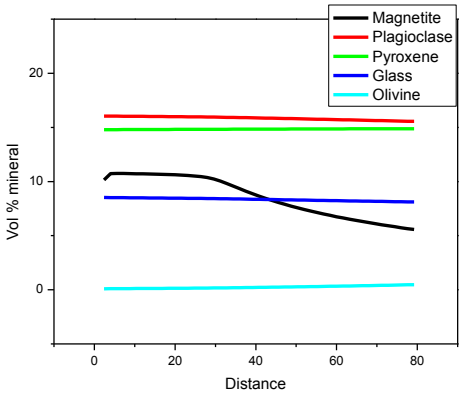

Figure 2*. Model outputs of a Rocknest eolian deposit-like parent material altered at a pH of 7 showing the absence of olivine, the preservation of other primary minerals, and the formation of magnetite. These results are consistent with CheMin measurements of the Big Sky target, indicating that its formation is consistent with this type of near-neutral aqueous alteration of a Rocknest eolian deposit-like parent material.*

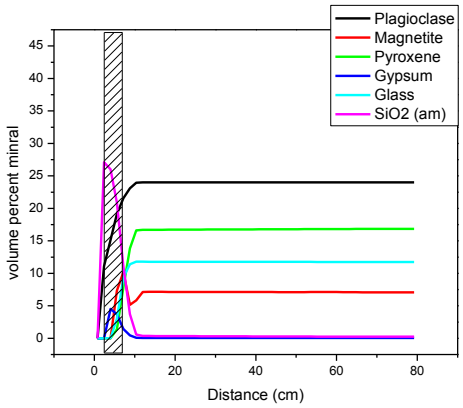

Figure 3. *Model outputs of a Big Sky target parent material altered under very acidic conditions (pH = 2). Results indicate dissolution of pyroxene, greater preservation of plagioclase, and precipitation of amorphous silica and gypsum in the region indicated by the hatched area, which is comparable to observations of the Greenhorn target.*

Conclusions:

Our modeling results help constrain the characteristics of at least two separate aqueous events impacting Gale Crater, Mars. Modeling results indicate that formation of Big Sky is consistent with aqueous alteration of a Rocknest eolian deposit-like parent material under pH conditions of ~6-8. Formation of Greenhorn is consistent with the weathering front generated under very acidic conditions (pH = ~2-4). Comparison of model times also indicates that the environmental conditions that formed Big Sky likely lasted significantly longer than the aqueous conditions that formed Greenhorn. These results help illuminate the complicated aqueous history of Mars.

References: 1.Grotzinger, J.P., et al., (2014) *Sci.*, *343* 1242777. 2. Rampe, E.B. et al. (submitted) *EPSL* 3. Ming, D.W., et al., (2016) *GSA Abstracts* doi: 10.1130/abs/2016AM-279126. 4. Yen, A.S., et al., *47th LPSC* 2016, Abstract #1649. 5. Steefel, C.I., *CrunchFlow* 2010: Berkeley, CA. www.steefel.com. 6. Hausrath, E.M., et al., (2008) *Geology*, *36* 67-70. 7. Navarre-Sitchler, A., et al., (2009) JGR., *114*. 8. Navarre-Sitchler, A., et al., (2011) *GCA 75* 7644-7667. 9. Maher, K., et al., (2009) *GCA 73* 2804-2831. 10. Maher, K., et al., (2006) *GCA 70* 337-363. 11. Maher, K., (2010) *EPSL 294* 101-110. 12. Hausrath, E.M. and A.A. Olsen, (2013) *AM*, *98* 897-906. 13. Adcock, C.T. and E.M. Hausrath, (2015) *Astro.*, *15* 1060-1075. 14. Gainey, S.R., et al. (in revision) *JGR* 15. Chadwick, O.A.et al. (1990) *Geomorph.*, *3* 369-390. 16. Houseknecht, D.W., (1987) *AAPG Bulletin*, *71* 633-642. 17. Bish, D.L., et al.,

(2013) *Sci*, *341*. 18. Wilson, A.M., et al. (2000) *GSA Bulletin*, *112* 845-856.